Theoretical Chemistry Accounts (2019) 138:65
https://doi.org/10.1007/s00214-019-2436-z

REGULAR ARTICLE

Theoretical determination of the OH-initiated oxidation rate constants of α, ω-dialkoxyfluoropolyethers

Luís P. Viegas[1]

Received: 10 January 2019 / Accepted: 12 March 2019 / Published online: 6 May 2019

Abstract

In this work, we have calculated rate constants for the tropospheric reaction between the OH radical and two α, ω-dialkoxyfluoropolyethers, namely $R-(OCF_2)_2-OR$, with $R=C_2H_5$ and $CH(CH_3)_2$. In terms of low atmospheric impact, dialkoxyfluoropolyethers are considered to be a promising class of the hydrofluoropolyethers family, although very little is still known about their reactivity. Calculation of the rate constants for these challenging molecular systems was performed by utilizing a cost-effective protocol for bimolecular hydrogen abstraction reactions based on multiconformer transition state theory and employing computationally feasible M08-HX electronic structure calculations. Within the protocol's uncertainties and approximations, the results maintain the tendencies of our own previous work: (1) OH-initiated oxidation rate constants of dialkoxyfluoropolyethers involving the ethyl and isopropyl groups have the same order of magnitude, which in turn is approximately 10 times larger than the rate constants involving dimethoxyfluoropolyethers; (2) the branching ratios concerning the α-hydrogens are much larger than the ones concerning the β-hydrogens; and (3) the chain length is seen to have a small effect on the rate constant, which is consistent with experimental work.

Keywords Atmospheric chemistry · Conformational sampling · Transition state theory · Density functional theory · Hydrofluoropolyethers

1 Introduction

On October 2016, almost 200 nations adopted the Kigali Amendment to the Montreal Protocol, a deal which is meant to phase-down production and use of hydrofluorocarbons (HFCs) and thought of having a decisive contribution to keep the global temperature rise under 2 °C, a target agreed at the Paris climate conference of 2015. HFCs, which are largely used [1] as second-generation replacements to the environmental hazardous CFCs [2–7], possess elevated values of global warming potential [8] (GWP), therefore contributing to the global warming problem addressed in the Paris and Kigali meetings. Hydrofluoroethers (HFEs) and hydrofluoropolyethers (HFPEs) are considered and recommended as an alternative [9–15] to be used as third-generation replacements because of their zero ozone depletion potential (ODP) and low GWP [13, 16–21].

Tropospheric oxidant attack by OH radicals is considered to be the main degradation pathway of oxygenated volatile organic compounds (OVOCs) [22–25]. However, there is not a great deal of research on the atmospheric chemistry aspects of the mechanisms, kinetics and reactivity of HFPEs toward the OH radical [17, 26–32].

HFPEs represent a family of linear oligomeric fluorinated compounds with the generic formula of [14]

$$R-(OCF_2CF_2)_p(OCF_2)_q-OR \quad (1)$$

where p and q define the number of repeating monomeric units. When R is chosen to be an alkyl substituent, these HFPEs are called α, ω-dialkoxyfluoropolyethers (DA-FPEs) and are considered to be promising in terms of having low

Published as part of the special collection of articles derived from the 11th Congress on Electronic Structure: Principles and Applications (ESPA-2018).

Electronic supplementary material The online version of this article (https://doi.org/10.1007/s00214-019-2436-z) contains supplementary material, which is available to authorized users.

✉ Luís P. Viegas
lpviegas@gmail.com

[1] Aarhus Institute of Advanced Studies, Aarhus University, Høegh-Guldbergs Gade 6B, Buildings 1630-1632, 8000 Aarhus, Denmark

atmospheric impact [27, 30–36]. Previous investigations concerning the calculation of these rate constants for DA-FPEs are extremely limited [27, 31, 32], with experimental work [27] solely focusing on α,ω-dimethoxyfluoropolyethers (DM-FPEs) [37, 38], which are obtained when R=CH_3. This class has been developed as potential CFC replacement for foaming and fire extinguishing agents, cleaning agents for sophisticated electronic devices and heat transfer fluids [27, 34, 36, 39, 40]. Regarding its atmospheric degradation, it has been claimed [27, 30, 36, 37] that the extra reactive sites for OH radical attack provided by the CH_3 groups in DM-FPEs are advantageous in limiting their atmospheric lifetimes, hence reducing GWP. A very recent investigation [31] has shed new light on this subject, suggesting that the reactivity patterns of DA-FPEs toward OH are mainly related to the barrier heights involving only the α-hydrogens on the alkyl groups, i.e., to the chemical environment at the α-carbons. As a consequence, branching ratios for the α-hydrogens were also shown to be much larger than for β and γ-hydrogens: $\Gamma_{\alpha}^{\mathrm{R}} \gg \Gamma_{\beta,\gamma}^{\mathrm{R}}$ for R = C_2H_5, C_3H_7 and $CH(CH_3)_2$.

Reactions between OH and HFPEs can be represented by the following generic equation:

$$\mathrm{R{-}(OCF_2CF_2)_p(OCF_2)_q{-}OR + OH} \xrightarrow{k_{pq}^{\mathrm{R}}} \text{ products} \tag{2}$$

In order to solidify our understanding of the reactivity patterns of DA-FPEs, we have chosen to extend our studies by considering a longer perfluoropolyether chain ($p0q2$ instead of $p0q1$ of ref [31]) and two specific R terminating groups: R=C_2H_5 and $CH(CH_3)_2$, which simplifies the above equation to

$$\mathrm{R{-}(OCF_2)_2{-}OR + OH} \xrightarrow{k_{02}^{\mathrm{R}}} \text{ products} \tag{3}$$

with associated rate constants $k_{02}^{\mathrm{C_2H_5}}$ and $k_{02}^{\mathrm{CH(CH_3)_2}}$.

The calculations were performed employing a cost-effective protocol [31] developed for bimolecular reactions and based on multiconformer transition state theory (MC-TST) [41–44]. Such methodology has been successfully used very recently in the calculation of complex cases of reaction (2), namely $p0q2$, $p0q3$ and $p2q0$ for R=CH_3 [32]. The computational details of such procedure will be given in the next section, and the results and discussion are subsequently presented. The conclusions are gathered in the last section.

2 Computational methods

In order to calculate the rate coefficients associated with reaction (3), some considerations should be made beforehand. We start by stating that the reactions between HFPEs and OH share mechanistic details found in many radical–molecule reactions of atmospheric interest (see Refs. [45, 46] and references therein), namely a reaction path in which there is the formation of pre-reactive complexes (PRC) and product complexes (PC) connected to the hydrogen abstraction transition states (TS). Such reaction path has been presented in detail in previous work [31, 32]. We should also state that HFPEs are known to have a rich conformational variety [31, 32, 47–49]. Including such conformational richness in the transition state theory equations [50] leads to MC-TST [31, 41–44] or to improvements and extensions to variational TST [Refs. [51, 52] and references therein]. For the bimolecular reactions here studied, the MC-TST equation can be written as [31]

$$k_{pq}^{\mathrm{R}} = \kappa(T)\frac{k_{\mathrm{B}}T}{hQ_{\mathrm{OH}}}\frac{\sum_i^M \frac{\alpha_i\omega_{\mathrm{TS}_i}Q_{\mathrm{TS}_i}}{\sigma_{\mathrm{rot,TS}_i}}}{\sum_j^N \frac{\alpha_j\omega_{\mathrm{HFPE}_j}Q_{\mathrm{HFPE}_j}}{\sigma_{\mathrm{rot,HFPE}_j}}}\mathrm{e}^{-V^{\ddagger}/k_{\mathrm{B}}T}. \tag{4}$$

Here, the Q's represent the partition functions for reactants and transition states, which are evaluated for translational, electronic, vibrational and rotational energies with $Q = q_{\mathrm{t}}q_{\mathrm{e}}q_{\mathrm{v}}q_{\mathrm{r}}$. The sum in the denominator of Eq. (4) runs through the total number of N available HFPE conformers, while the numerator runs through all possible (M) available transition state conformers [31, 42, 50] which are accounted by considering an OH attack on each hydrogen atom of a particular HFPE conformer [31, 32]. Thus, M is found by multiplying the number of hydrogen atoms of each HFPE conformer by the total number of HFPE conformers, $M = n_{\mathrm{H}} \times N$. For the two cases presented in this work, we will have $n_{\mathrm{H}} = 10$ and 14 for R = C_2H_5 and $CH(CH_3)_2$, respectively. The quantities represented by $\omega_{\mathrm{HFPE}_j} = \mathrm{e}^{-(E_{\mathrm{HFPE}_j}-E_{\mathrm{HFPE}_0})/k_{\mathrm{B}}T} = \mathrm{e}^{-\Delta E_{\mathrm{HFPE}_j}/k_{\mathrm{B}}T}$, $\omega_{\mathrm{TS}_i} = \mathrm{e}^{-(E_{\mathrm{TS}_i}-E_{\mathrm{TS}_0})/k_{\mathrm{B}}T} = \mathrm{e}^{-\Delta E_{\mathrm{TS}_i}/k_{\mathrm{B}}T}$, $\sigma_{\mathrm{rot,HFPE}_j}$, $\sigma_{\mathrm{rot,TS}_i}$, α_j and α_i are the thermal weight factors, rotational symmetry numbers [42] and reaction path degeneracy parameters [31] of conformations HFPE_j and TS_i, respectively. The zero-point energy (ZPE)-corrected energy of conformations HFPE_j and TS_i is represented by E_{HFPE_j} and E_{TS_i}. The quantity $V^{\ddagger}$ is calculated as $V^{\ddagger} = E_{\mathrm{TS}_0} - (E_{\mathrm{HFPE}_0} + E_{\mathrm{OH}})$ and represents the difference between the ZPE-corrected energy of the most stable transition state conformation and the ZPE-corrected energy of the most stable reactants [31, 42, 44, 50]. Finally, $\kappa(T)$ is the tunneling correction associated with the lowest energy TS, calculated through the Eckart method [53], widely used in atmospheric chemistry studies [44, 50, 54–68].

The necessary electronic structure calculations were performed with the GAMESS package [69], with the choice of model chemistry being made according to our own cost-effective philosophy [31, 49]. We have utilized the M08-HX/

apcseg-2//M08-HX/pcseg-1 model chemistry, with the optimizations and single-point energies being performed with M08-HX [70] from the Minnesota family of functionals and with Jensen's [71] new segmented polarization consistent double- and triple-ζ basis sets.

Our choice of opting for DFT calculations relies on the fact that they can be accurate while having a low CPU time scaling (typically around K^4, where K is a measure of the size of the molecule), a very important feature concerning calculations on increasingly complex HFPEs. On the other hand, the Minnesota family of functionals is used with good accuracy in many research investigations concerning the reactivity of VOCs [47, 65, 67, 72–83]. Although M06-2X [84] is more frequently used than M08-HX [70], we point out that for hydrogen transfer barrier heights, M08-HX has a mean unsigned error (MUE) 0.2 kcal mol^{-1} lower than M06-2X for the DBH76 data set [85–87] and 0.4 kcal mol^{-1} lower than M06-2X for the HTBH38 data set, a component of DBH76 [84, 88]. The more recent M11 [89] functional has a MUE for the HTBH38 data set almost 0.6 kcal mol^{-1} higher than M08-HX. Our previous calculations [49] also reveal that M06-2X and M08-HX yield similar geometries and relative energies for various DA-FPEs.

We performed the M08-HX calculations using the new segmented polarization consistent basis sets of Jensen [71] without (pcseg-*n*) and with diffuse augmentation (aug-pcseg-*n*), which have been optimized for DFT methods. These basis sets represent not only an improvement (both in accuracy and in computational efficiency) to the previous polarization consistent (pc-*n*) basis sets [90–94] but also a low error alternative to several other basis sets [71], regarding DFT calculations. It was also shown [71] that the basis set errors of pcseg-*n* at a given ζ quality level are lower than other existing basis sets while being among the computationally most efficient.

The $V^{\ddagger}$ barrier height and the $\kappa(T)$ tunneling factor were also calculated at the more expensive M08-HX/apcseg-2//M08-HX/pcseg-2 level of theory in order to have an error bar associated with the rate constants.

The several steps and details making up our cost-effective protocol have been carefully described in our previous work [31, 32], and the reader is referred to those publications for a more in-depth analysis.

3 Results and discussion

One of the important aspects of the aforementioned protocol [31] is the reduction in the number of necessary electronic structure calculations. This relates directly to the magnitude of the N and M indexes of Eq. (4). In the particular case of the calculations performed in this work, the reduction in the number of DA-FPE conformers originating from the removal of duplicates and enantiomers after conformer generation is minimal: 3 and 5% for R=C_2H_5 and $CH(CH_3)_2$, respectively. This reduction was achieved by performing a similarity evaluation (SE) step [31], which consists of running a pairwise comparison between all generated DA-FPE conformers using a superimposing algorithm [95] and evaluating geometrical similarity by minimizing the sum over all distances between each corresponding atom in a pair of structures. The SE step is applied only to the reactants [31], since it is assumed that each OH attack on a unique DA-FPE conformer will originate a unique TS structure. The reduction in the number of TS conformers, which will be explained next, is quite considerable and essential in lowering the computational effort: 71 and 79% for R=C_2H_5 and $CH(CH_3)_2$, respectively. This means that for R=C_2H_5 we have $N = 229$ and $M = 670$, while for $CH(CH_3)_2$ we end up with $N = 218$ and $M = 686$. Note that if we wanted to generate all possible TS conformers, then M would have the values of 2290 and 3052 for R=C_2H_5 and $CH(CH_3)_2$, respectively. This reduction was achieved by ordering the DA-FPE conformers by ZPE-corrected energy and generating the TS conformers from the set of DA-FPEs that summed up to 90% of the total fractional population. Such an approach was shown to introduce a low error on the final rate constants [31] while achieving major computational savings by reducing the number of TS optimizations [31, 32], as it is also the case in the present investigation.

We now present the two IRC paths connecting the TS to PRC and PC for the studied cases, calculated at the M08-HX/pcseg-1 level (Fig. 1) along with the necessary data to calculate both tunneling factors (Table 1). It can be observed that the tunneling factors decrease with the size of the R alkyl substituent. This is essentially related to the values of the imaginary frequency of the transition states and

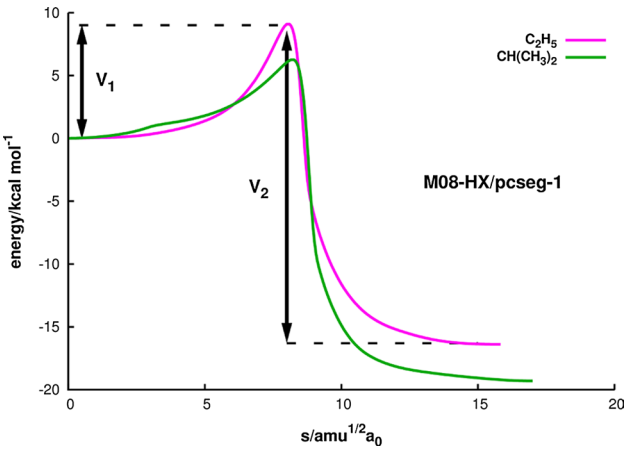

Fig. 1 Full IRC paths for the R=C_2H_5 and $CH(CH_3)_2$ cases, calculated at the M08-HX/pcseg-1 level of theory and plotted with respect to each of the PRC ($s = 0$ amu$^{1/2}$ a$_0$)

Table 1 Necessary data to calculate the κ_{02}^{R} tunneling factors: imaginary frequencies of the transition states ($\nu^{\ddagger}$, in cm^{-1}, calculated at the M08-HX/pcseg-1 level) and forward and reverse barrier heights (V_1 and V_2, in kcal mol^{-1}, calculated at the M08-HX/apcseg-2//M08-HX/pcseg-1 level)

R	$\nu^{\ddagger}$	V_1	V_2	κ_{02}^{R}	References
CH_3	1164.2	4.9	23.2	3.8	[32]
C_2H_5	1066.7	5.0	25.2	3.2	This work
$CH(CH_3)_2$	831.4	2.6	25.4	1.8	This work

becomes even more evident by comparing these numbers to the ones making up the $\kappa_{02}^{CH_3}$ case [32]. This progressive decrease in the imaginary frequencies was shown [31] to be related to the reduction in the inductive effects [6, 12, 47, 48, 96] felt by the abstracted hydrogen atom, which can also be used to rationalize the increasing values of the perpendicular looseness [97] (sum of the making and forming bond distances): 2.54 Å for R=CH_3 [32], 2.57 and 2.60 Å for R=C_2H_5 and $CH(CH_3)_2$, respectively.

The MC-TST rate constants for the two reactions studied in this work are collected in Table 2, along with the value of $k_{02}^{CH_3}$(MC -TST) [32]. It can be seen that replacing the methyl groups by ethyl groups increases the rate constant by more than twenty times, but a replacement by the isopropyl groups leads to a lower increase of slightly over ten times. A similar behavior is observed for the $p0q1$ case [31], and this will be explored in more detail in future work when all calculations for R=CF_2H are available. We should stress that the error bars of Table 2 are obtained by observing the effect of calculating $V^{\ddagger}$ and $\kappa(T)$ at the M08-HX/apcseg-2//M08-HX/pcseg-2 level of theory, which will ultimately affect the rate constants [31, 32]. However, it should be noted that the M08-HX functional has a MUE of 1 kcal mol^{-1} for the DBH76 data set [70]. Using this value as a systematic error in the barrier heights, the errors bars for $k_{02}^{C_2H_5}$ and $k_{02}^{CH(CH_3)_2}$ become 2.3×10^{-13} and 1.3×10^{-13} cm^3 $molecule^{-1}$ s^{-1}, respectively.

In order to better understand the effect of increasing the chain length from $p0q1$ to $p0q2$ for the R=C_2H_5 and $CH(CH_3)_2$ cases, we have used our own approach [32] for the R=CH_3 case, where we fix R and calculate the ratio between the "long-chain" rate constant and the "short-chain" one that we consider as reference. Here, we will take k_{01}^{R} as the reference and calculate the two ratios as

$$\eta_{02}^{R}(\text{MC-TST}) = \frac{k_{02}^{R}(\text{MC-TST})}{k_{01}^{R}(\text{MC-TST})}. \quad (5)$$

This equation can be written in a way [31, 32] we can distinguish its three different contributions originating from Eq. (4)

$$\eta_{02}^{R}(\text{MC-TST}) = \frac{\kappa_{02}^{R}}{\kappa_{01}^{R}} \frac{Q_{02}^{R}(90\%)}{Q_{01}^{R}(90\%)} \frac{\Delta_{02}^{R}}{\Delta_{01}^{R}} \quad (6)$$

with the first term concerning the ratio between tunneling factors, the second term concerning just the ratio between the sums of Eq. (4) and the third term concerning the ratio between the terms involving the exponential function containing the barrier heights. The results for η and their different contributions are given in Table 3, where we also include the $\eta_{02}^{CH_3}$ case [32] for clarity. Interestingly, both η values calculated in this work are the same, which means that increasing the chain length from $p0q1$ to $p0q2$ reduces the rate constant by a factor of 0.41 for both R = C_2H_5 and $CH(CH_3)_2$ cases. However, such an agreement is seen to be fortuitous, as the three contributions for each of the η values are considerably different. Such a fortuitous agreement in the η values is also seen [32] between $\eta_{02}^{CH_3}$ and $\eta_{03}^{CH_3}$, which of course leads to the question of what will happen to the $\eta_{03}^{C_2H_5}$ and $\eta_{03}^{CH(CH_3)_2}$ cases. The close agreement between $k_{02}^{CH_3}$ and $k_{03}^{CH_3}$ [32], although seen to be fortuitous by inspection of the three contributions to the η values, seems to suggest that increasing the chain length from $p0q2$ to $p0q3$ could also leave the rate constants practically unchanged for R=C_2H_5 and $CH(CH_3)_2$ cases. Testing this hypothesis would require time-consuming calculations that remain outside the scope of our present objectives, at least for the time being.

In terms of the importance of which carbon sites determine $V^{\ddagger}$, it is seen that the chemical environment in the α -carbons defines the barrier height and the higher reactivity of the compounds with R=C_2H_5 and $CH(CH_3)_2$ [31]. Such a claim is supported not only by the values of the branching ratios ($\Gamma_{\alpha,\beta}^{R}$) concerning the hydrogen abstractions at the α

Table 2 MC-TST rate constants for the reaction between the OH radical and R−$(OCF_2)_2$−OR calculated at 298.15 K

R	k_{02}^{R} (cm^3 $molecule^{-1}$ s^{-1})	References
CH_3	$(1.3 \pm 0.2) \times 10^{-14}$	[32]
C_2H_5	$(2.8 \pm 0.2) \times 10^{-13}$	This work
$CH(CH_3)_2$	$(1.6 \pm 0.5) \times 10^{-13}$	This work

Table 3 The three contributions for η_{02}^{R} (see Eq. (6) and text) and its final value

R	$\frac{\kappa_{02}^{R}}{\kappa_{01}^{R}}$	$\frac{Q_{02}^{R}(90\%)}{Q_{01}^{R}(90\%)}$	$\frac{\Delta_{02}^{R}}{\Delta_{01}^{R}}$	η_{02}^{R}	References
CH_3	1.37	0.41	0.45	0.25	[32]
C_2H_5	1.46	0.61	0.47	0.41	This work
$CH(CH_3)_2$	1.02	0.20	2.01	0.41	This work

and β carbons ($\Gamma_{\alpha}^{C_2H_5} = 97\%$, $\Gamma_{\beta}^{C_2H_5} = 3\%$ and $\Gamma_{\alpha}^{CH(CH_3)_2} = 78.8\%$ and $\Gamma_{\beta}^{CH(CH_3)_2} = 21.2\%$), but also with the values of the lowest barrier heights of each type of hydrogen [31, 76] ($V_{\alpha,\beta}^{\ddagger,R}$), calculated at the M08-HX/apcseg-2//M08-HX/pcseg-1 level: $V_{\alpha}^{\ddagger,C_2H_5} = 0.47$, $V_{\beta}^{\ddagger,C_2H_5} = 1.40$; $V_{\alpha}^{\ddagger,CH(CH_3)_2} = -1.17$, $V_{\beta}^{\ddagger,CH(CH_3)_2} = 0.63$ kcal mol^{-1}.

3.1 Atmospheric lifetimes

The atmospheric lifetime of DA-FPEs will be determined by their reaction with OH radicals. By using a value of $[OH] = 1 \times 10^6$ molecules cm^{-3} for the global average concentration [98], the tropospheric lifetimes can be estimated via $\tau_{02}^{R} = 1/k_{02}^{R}[OH]$. Using the calculated MC-TST rate constants, we obtain the following lifetimes: $\tau_{02}^{C_2H_5} \approx 41$ days and $\tau_{02}^{CH(CH_3)_2} \approx 72$ days.

4 Conclusions

In this investigation, we have calculated the theoretical rate constants for the reactions between two DA-FPEs and the OH radical. To our knowledge, it is the first time these rate coefficients ($k_{02}^{C_2H_5}$ and $k_{02}^{CH(CH_3)_2}$) are being reported. Due to the size and conformational complexity of these species, our calculations were performed within the framework of a cost-effective protocol for MC-TST based on DFT electronic structure calculations, developed to tackle challenging bimolecular hydrogen abstraction reactions such as the ones here presented. If one includes the $k_{02}^{CH_3}$ rate constant in the discussion, it can be concluded that: (1) OH-initiated oxidation rate constants of the DA-FPEs involving the ethyl and isopropyl groups have the same order of magnitude, which in turn is approximately 10 times larger than the corresponding rate constant for the dimethoxyfluoropolyether, $k_{02}^{CH_3}$; (2) the branching ratios concerning the α-hydrogens are much larger than the ones concerning the β-hydrogens; and (3) within the protocol's uncertainties and approximations, the chain length is seen to have a small effect on the rate constant, which is consistent with experimental work performed on DM-FPEs. We stress that items (1) and (2), which concern the present $p0q2$ case, are consistent with the equivalent reactions for the $p0q1$ case [31].

The work here presented represents the toughest challenge so far to this cost-effective protocol, and it shows its practical predictive ability. An extension of this study for the $p0q3$ (and even $p0q4$) would of course be welcomed, but we should point out that even considering all simplifications (for example, optimizing less than 30% of the possible TS conformers) and using 16-, 20-, 24-, 28- and 36-core servers, the optimizations and single-point energy calculations for this work alone amounted to a total wall clock time equivalent to 10 and 22 months of uninterrupted calculations for R=C_2H_5 and $CH(CH_3)_2$, respectively.

Acknowledgements L.P.V. acknowledges financial support from the AIAS-COFUND Marie Curie program (Grant Agreement No. 609033), Prof. Frank Jensen for providing access to the computational resources and for the insightful discussions and also Dr. Serguei Patchkovskii for the brute force symmetry determination program.

References

1. Montzka S, Reimann S, Engel A, Krüger K, O'Doherty S, Sturges W (2011) Ozone-depleting substances (ODSs) and related chemicals, Chapter 1, scientific assessment of ozone depletion: 2010, global ozone research and monitoring project-report no. 52. World Meteorological Organization, Geneva
2. Molina MJ, Rowland FS (1974) Nature 249:810
3. Farman JD, Gardiner BG, Shanklin JD (1985) Nature 315:207
4. Montreal protocol on substances that deplete the ozone layer. Final Act, UNEP, 1987 (Revised 1990, London Amendment; revised 1992, Copenhagen Amendment)
5. Zurer PS (1993) Chem Eng News 71:8–18
6. Lazarou YG, Papagiannakopoulos P (1999) Chem Phys Lett 301:19
7. The Kyoto Protocol to the United Nations Framework Convention on Climate Change (UNFCCC) (1997)
8. UNEP (2011) HFCs: a critical link in protecting climate and the ozone layer. United Nations Environment Programme (UNEP), Nairobi, p 36
9. Zhang Z, Saini RD, Kurylo MJ, Huie RE (1992) J Phys Chem 96:9301
10. Hsu KJ, DeMore WB (1995) J Phys Chem 99:11141
11. Wallington TJ, Schneider WF, Sehested J, Bilde M, Platz J, Nielsen OJ, Christensen LK, Molina MJ, Molina LT, Wooldridge PW (1997) J Phys Chem A 101:8264
12. Kambanis KG, Lazarou YG, Papagiannakopoulos P (1998) J Phys Chem A 102:8620
13. Marchionni G, Silvani R, Fontana G, Malinverno G, Visca M (1999) J Fluor Chem 95:41
14. Tsai WT (2007) J Hazard Mater A 139:185
15. Bravo I, Marston G, Nutt DR, Shine KP (2011) J Quant Spectrosc Radiat Transfer 112:1967
16. Bivens DB, Minor BH (1998) Int J Refrig 21:567
17. Cavalli F, Glasius M, Hjorth J, Rindone B, Jensen NR (1998) Atmos Environ 32:3767
18. Sekiya A, Misaki S (2000) J Fluor Chem 101:215
19. Urata S, Takada A, Uchimaru T, Chandra AK (2003) Chem Phys Lett 368:215
20. Østerstrøm FF, Nielsen OJ, Andersen MPS, Wallington TJ (2012) Chem Phys Lett 524:32
21. Blanco MB, Rivela C, Teruel MA (2013) Chem Phys Lett 578:33
22. Mellouki A, Le Bras G, Sidebottom H (2003) Chem Rev 103:5077
23. Vereecken L, Francisco JS (2012) Chem Soc Rev 41:6259
24. Mellouki A, Wallington TJ, Chen J (2015) Chem Rev 115:3984
25. Vereecken L, Aumont B, Barnes I, Bozzelli JW, Goldman MJ, Green WH, Madronich S, McGillen MR, Mellouki A, Orlando JJ, Picquet-Varrault B, Rickard AR, Stockwell WR, Wallington TJ, Carter WPL (2018) Int J Chem Kinet 50:435
26. Tuazon EC (1997) Environ Sci Technol 31:1817
27. Andersen MPS, Hurley MD, Wallington TJ, Blandini F, Jensen NR, Librando V, Hjorth J, Marchionni G, Avataneo M, Visca M, Nicolaisen FM, Nielsen OJ (2004) J Phys Chem A 108:1964

28. Wallington TJ, Hurley MD, Javadi TS, Nielsen OJ (2008) Int J Chem Kinet 40:819
29. Andersen MPS, Andersen VF, Nielsen OJ, Sander SP, Wallington TJ (2010) ChemPhysChem 11:4035
30. Menghua W, Navarrini W, Avataneo M, Venturini F, Sansotera M, Gola M (2011) Chimica Oggi 29:67
31. Viegas LP (2018) J Phys Chem A 122:9721
32. Viegas LP (2019) Int J Chem Kinet. https://doi.org/10.1002/kin.21259
33. Marchionni G, Guarda PA (1998) US Patent 5,744,651
34. Marchionni G, Visca M (2003) Eur Pat Appl EP1275678A2
35. Navarrini W, Galimberti M, Fontana G (2006) US Patent 7,141,704
36. Wu M, Navarrini W, Spataro G, Venturini F, Sansotera M (2012) Appl Sci 2:351
37. Marchionni G, Avataneo M, De Patto U, Maccone P, Pezzin G (2005) J Fluor Chem 126:465
38. Avataneo M, De Patto U, Galimberti M, Marchionni G (2005) J Fluor Chem 126:631
39. Marchionni G, Maccone P, Pezzin G (2002) J Fluor Chem 118:149
40. Marchionni G, Petricci S, Guarda PA, Spataro G, Pezzin G (2004) J Fluor Chem 125:1081
41. Vereecken L, Peeters J (2003) J Chem Phys 119:5159
42. Fernández-Ramos A, Ellingson BA, Meana-Pañeda R, Marques JMC, Truhlar DG (2007) Theor Chem Acc 118:813
43. Petit AS, Harvey JN (2012) Phys Chem Chem Phys 14:184
44. Rissanen MP, Kurtén T, Sipilä M, Thornton JA, Kangasluoma J, Sarnela N, Junninen H, Jørgensen S, Schallhart S, Kajos MK, Taipale R, Springer M, Mentel TF, Ruuskanen T, Petäjä T, Worsnop DR, Kjaergaard HG, Ehn M (2014) J Am Chem Soc 136:15596
45. Hansen JC, Francisco JS (2002) ChemPhysChem 3:833
46. Hernández-Soto H, Weinhold F, Francisco JS (2007) J Chem Phys 127:164102
47. Radice S, Causà M, Marchionni G (1998) J Fluor Chem 88:127
48. Radice S, Toniolo P, Avataneo M, De Patto U, Marchionni G, Castiglioni C, Tommasini M, Zerbi G (2004) J Mol Struct Theor Chem 710:151
49. Viegas LP (2017) Int J Quantum Chem 117:e25381
50. Møller KH, Otkjaer RV, Hyttinen N, Kurtén T, Kjaergaard HG (2016) J Phys Chem A 120:10072
51. Bao JL, Truhlar DG (2017) Chem Soc Rev 46:7548
52. Ferro-Costas D, Martínez-Núñez E, Rodríguez-Otero J, Cabaleiro-Lago E, Estévez CM, Fernández B, Fernández-Ramos A, Vázquez SA (2018) J Phys Chem A 122:4790
53. Eckart C (1930) Phys Rev 35:1303
54. Mora-Diez N, Alvarez-Idaboy JR, Boyd RJ (2001) J Phys Chem A 105:9034
55. Alvarez-Idaboy JR, Mora-Diez N, Boyd RJ, Vivier-Bunge A (2001) J Am Chem Soc 123:2018
56. Galano A, Alvarez-Idaboy JR, Ruiz-Santoyo ME, Vivier-Bunge A (2002) J Phys Chem A 106:9520
57. Bravo-Pérez G, Alvarez-Idaboy JR, Cruz-Torres A, Ruíz ME (2002) J Phys Chem A 106:4645
58. Galano A, Alvarez-Idaboy JR, Bravo-Pérez G, Ruiz-Santoyo ME (2002) Phys Chem Chem Phys 4:4648
59. Alvarez-Idaboy JR, Cruz-Torres A, Galano A, Ruiz-Santoyo ME (2004) J Phys Chem A 108:2740
60. Bravo-Pérez G, Alvarez-Idaboy JR, Jiménez AG, Cruz-Torres A (2005) Chem Phys 310:213
61. Cruz-Torres A, Galano A, Alvarez-Idaboy JR (2006) Phys Chem Chem Phys 8:285
62. Iuga C, Alvarez-Idaboy JR, Reyes L, Vivier-Bunge A (2010) J Phys Chem Lett 1:3112
63. Iuga C, Alvarez-Idaboy JR, Vivier-Bunge A (2011) Theor Chem Acc 129:209
64. Zhang F, Dibble TS (2011) Phys Chem Chem Phys 13:17969
65. de la Luz AP, Iuga C, Alvarez-Idaboy JR, Ortíz E, Vivier-Bunge A (2012) Int J Quantum Chem 112:3525
66. Elm J, Jørgensen S, Bilde M, Mikkelsen KV (2013) Phys Chem Chem Phys 15:9636
67. Bänsch C, Kiecherer J, Szöri M, Olzmann M (2013) J Phys Chem A 117:8343
68. Kurtén T, Rissanen MP, Mackeprang K, Thornton JA, Hyttinen N, Jørgensen S, Ehn M, Kjaergaard HG (2015) J Phys Chem A 119:11366
69. Schmidt MW, Baldridge KK, Boatz JA, Elbert ST, Gordon MS, Jensen JH, Koseki S, Matsunaga N, Nguyen KA, Su S, Windus TL, Dupuis M, Montgomery JA Jr (1993) J Comput Chem 14:1347
70. Zhao Y, Truhlar DG (2008) J Chem Theory Comput 4:1849
71. Jensen F (2014) J Chem Theory Comput 10:1074
72. Bottoni A, Della Casa P, Poggi G (2001) J Mol Struct Theor Chem 542:123
73. Atadinç F, Selçuki C, Sari L, Aviyente V (2002) Phys Chem Chem Phys 4:1797
74. Wu JY, Liu JY, Li ZS, Sun CC (2003) J Chem Phys 118:10986
75. El-Nahas AM, Uchimaru T, Sugie M, Tokuhashi K, Sekiya A (2005) J Mol Struct Theor Chem 722:9
76. Zavala-Oseguera C, Alvarez-Idaboy JR, Merino G, Galano A (2009) J Phys Chem A 113:13913
77. Zhou CW, Simmie JM, Curran HJ (2010) Phys Chem Chem Phys 12:7221
78. Yu T, Zheng J, Truhlar DG (2011) Chem Sci 2:2199
79. Yu T, Zheng J, Truhlar DG (2012) J Phys Chem A 116:297
80. Zheng J, Seal P, Truhlar DG (2013) Chem Sci 4:200
81. Ramasami P, Abdallah HH, Archibong EF, Blowers P, Ford TA, Kakkar R, Shuai Z, Schaefer HF III (2013) Pure Appl Chem 85:1901
82. Balaganesh M, Rajakumar B (2014) J Mol Graph Model 48:60
83. Jørgensen S, Knap HC, Otkjaer RV, Jensen AM, Kjeldsen MLH, Wennberg PO, Kjaergaard HG (2016) J Phys Chem A 120:266
84. Zhao Y, Truhlar DG (2008) Theor Chem Acc 120:215
85. Zhao Y, Schultz NE, Truhlar DG (2006) J Chem Theory Comput 2:364
86. Zhao Y, González-Garcia N, Truhlar DG (2005) J Phys Chem A 109:2012
87. Zhao Y, Lynch BJ, Truhlar DG (2005) Phys Chem Chem Phys 7:43
88. Zhao Y, Truhlar DG (2006) J Chem Phys 125:194101
89. Peverati R, Truhlar DG (2011) J Phys Chem Lett 2:2810
90. Jensen F (2001) J Chem Phys 115:9113
91. Jensen F, Helgaker T (2004) J Chem Phys 121:3463
92. Jensen F (2007) J Phys Chem A 111:11198
93. Jensen F (2012) J Chem Phys 136:114107
94. Jensen F (2013) J Chem Phys 138:014107
95. Marques JMC, Llanio-Trujillo JL, Abreu PE, Pereira FB (2010) J Chem Inf Model 50:2129
96. Fontana G, Causà M, Gianotti V, Marchionni G (2001) J Fluor Chem 109:113
97. Lynch BJ, Truhlar DG (2001) J Phys Chem A 105:2936
98. Prinn RG, Huang J, Weiss RF, Cunnold DM, Fraser PJ, Simmonds PG, McCulloch A, Harth C, Salameh P, O'Doherty S, Wang RHJ, Porter L, Miller BR (2001) Science 292:1882